



HAL
open science

Reliability evaluation of automated analysis, 2D scanner, and micro-tomography methods for measuring fiber dimensions in polymer-lignocellulosic fiber composites

Erika Di Giuseppe, Romain Castellani, Simon Dobosz, Jérôme Malvestio, Françoise Berzin, Johnny Beaugrand, Christine Delisée, Bruno Vergnes, Tatiana Budtova

► To cite this version:

Erika Di Giuseppe, Romain Castellani, Simon Dobosz, Jérôme Malvestio, Françoise Berzin, et al.. Reliability evaluation of automated analysis, 2D scanner, and micro-tomography methods for measuring fiber dimensions in polymer-lignocellulosic fiber composites. *Composites Part A: Applied Science and Manufacturing*, 2016, 90, pp.320-329. 10.1016/j.compositesa.2016.07.020 . hal-02420034

HAL Id: hal-02420034

<https://hal.science/hal-02420034>

Submitted on 20 Mar 2023

HAL is a multi-disciplinary open access archive for the deposit and dissemination of scientific research documents, whether they are published or not. The documents may come from teaching and research institutions in France or abroad, or from public or private research centers.

L'archive ouverte pluridisciplinaire **HAL**, est destinée au dépôt et à la diffusion de documents scientifiques de niveau recherche, publiés ou non, émanant des établissements d'enseignement et de recherche français ou étrangers, des laboratoires publics ou privés.

Reliability evaluation of automated analysis, 2D scanner, and micro-tomography methods for measuring fiber dimensions in polymer-lignocellulosic fiber composites

Erika Di Giuseppe¹, Romain Castellani¹, Simon Dobosz^{2,3}, Jérôme Malvestio⁴, Françoise Berzin^{2,3}, Johnny Beaugrand^{2,3}, Christine Delisée⁴, Bruno Vergnes¹, Tatiana Budtova^{1*}

¹ *MINES ParisTech, PSL Research University, CEMEF (Centre for Material Forming), UMR CNRS 7635, CS 10207, 06904 Sophia Antipolis Cedex, France*

² *INRA, UMR614 FARE (Fractionnement des AgroRessources et Environnement), 2 esplanade Roland-Garros, 51686 Reims, France*

³ *Université de Reims Champagne-Ardenne, UMR614 FARE (Fractionnement des AgroRessources et Environnement), 2 esplanade Roland-Garros, 51686 Reims, France*

⁴ *Université de Bordeaux, I2M (Institut de Mécanique et Ingénierie), UMR 5295, 351 cours de la Libération, 33400 Talence, France*

Corresponding author:

T. Budtova, MINES ParisTech, PSL Research University, CEMEF, UMR CNRS 7635

Tatiana.budtova@mines-paristech.fr

Tel.: (+33) 493 95 7470

ABSTRACT

Composite processing strongly affects the size of lignocellulosic fibers, and consequently the mechanical properties of the final product. Using a reliable method for the analysis of fiber length and diameter distributions is thus crucial for the understanding of fiber behavior during processing. In this study, three different techniques, X-ray microtomography, 2D scanning and automated fiber analyzer, were compared in terms of their reliability for the characterization of dimensions of two kinds of lignocellulosic fibers, hemp and miscanthus, in polymer-natural fiber composites. Statistical analysis was employed to interpret fiber size distributions. The study confirmed that interpreting the dimensions of natural fiber is still a difficult task. The inherent limitations of the measuring methods make each technique complementary to the others in terms of length scale. The choice of the technique is, therefore, strictly dependent on fiber dimensions and the aim of the work.

Keywords: A. Natural fibers; A. Polymer-matrix composites; B. Microstructures; C. Statistical properties/methods

1. INTRODUCTION

In the last decades, the interest in using natural fibers in polymer composites has largely grown. Lignocellulosic fibers present lower density compared to conventional reinforcements, such as glass fibers, leading to lighter manufactured materials and displaying competitive mechanical properties [1]. Moreover, they come from renewable resources, are non-toxic and usually environmentally friendly [2].

The mechanical properties of fiber-reinforced composites are controlled by the efficiency of the stress transfer from the polymer matrix to the fibers. It depends on (i) the fiber/matrix adhesion, (ii) fibers dispersion and distribution in the matrix, (iii) the type and composition of the fibers, and (iv) their geometrical characteristics (length L , diameter D , aspect ratio L/D). The latter are, in turn, strongly affected by processing conditions. Contrarily to glass fibers that are

of a uniform diameter, lignocellulosic fibers are usually in bundles of elementary fibers assembled together. Stresses arising during processing may reduce not only the length of the fibers through breakage, but also bundles' diameter through dissociation into the elementary fibers. Fibers fibrillation may also occur. The measurement of the geometrical characteristics of the fibers is thus crucial to understand their breakage mechanisms and to predict the properties of a composite.

There is no international standard for the natural fiber dimensions measurement which is the open door for plenty of homemade solutions. Several major methods have been used, such as X-ray microtomography (X-ray μ -CT) [3- 6], optical microscopy [7- 10], fiber size analyzers [11, 12], 2D high-resolution scanners [13] and scanning electron microscopy (SEM) [14-16]. SEM technique is suitable for the evaluation of fiber diameters [14] and the characterization of the changes of surface features due to chemical treatments carried out to improve the fiber/matrix adhesion [15, 16]. However, it does not enable a good statistically representative quantification of fiber length.

To allow the measurement of fiber size distributions, the composite must be treated according to the method used. For example, it can be melted and compressed to obtain a thin film for the observations by optical microscopy [7]. Alternatively, the polymer matrix can be dissolved and the fibers (i) extracted in a Soxhlet apparatus and their sizes analyzed by an automated analyzer [12], or (ii) separated by centrifugation and analyzed by a scanner [13], or (iii) left suspended in dissolved matrix and analyzed by optical microscopy [8, 9]. Only the μ -CT does not require any specific sample preparation, but it needs quite expensive technical and computational investments for performing experiments and analyzing the data.

Once size measurements have been performed, it is necessary to obtain and interpret the fiber size distributions. A single number such as the arithmetic mean cannot describe precisely fiber size distributions that are usually very wide, from a few to several thousands of microns [9]. Size distributions are strongly affected (i) by the method with which the geometrical parameters are calculated, (ii) by the choice of the representative variables that describe the distributions, i.e. root mean square, arithmetic, or contraharmonic mean [12, 17] and (iii) by the

basis on which the data are presented (i.e. number, surface, volume) [6, 8, 9, 18]. Quantifying natural fiber dimensions is therefore a difficult task, which can obviously be influenced by several aspects, among which are the preparation of the samples for the observations and the measurements, the intrinsic limitations of the measuring technique, the procedure used for the image processing, and the employed statistical method [9, 12, 19].

In this work we investigated the reliability (advantages and limitations) of three different techniques that are commonly used for assessing size distributions of lignocellulosic fibers in polymer composites, i.e. X-ray microtomography, 2D scanning technique, and automated dynamic fiber analyzer. Two types of fibers with different morphology were chosen, hemp (RH) and miscanthus (M). Composites were made using a laboratory-scale co-rotating twin-screw extruder.

2. EXPERIMENTAL

2.1 Materials

The polymer matrix is a homopolymer polypropylene (PPH 5060) purchased from Total Petrochemicals (melt flow index, MFI, 6 g/10 min at 230 °C and 2.16 kg, melting temperature 164 °C and molar mass 320 000 g/mol). Maleic anhydride grafted-polypropylene (MA-g-PP), with a density of 910 kg/m³ and MFI > 50 g/10 min at 230 °C and 2.16 kg, was used as compatibilizer.

Two types of fibers of different morphology, kindly provided by FRD[®] corporation (Fibres Recherche Développement[®], Troyes, France) were used: i) Miscanthus from stem (M) and ii) retted hemp fibers *Cannabis sativa L.* (RH). The images of fibers before extrusion and within the composite are given in Fig. S1 (Supplementary Data). Fibers were stored at 20 °C and 50 % relative humidity before compounding. Two solvents were employed to dissolve the matrix: Decalin[®] (decahydronaphtalene, C₁₀H₁₈) was purchased from Fisher Chemical and used for scanner technique and p-xylene (C₈H₁₀) was purchased from Sigma-Aldrich and used for the automated fiber analysis.

2.2. Methods

2.2.1 Composite preparation

Composites were prepared on a laboratory-scale twin-screw extruder (Cleextral BC21, Firminy, France). The details are given in the Supplementary Data (Table S1). The PP and MA-g-PP (78/2 wt./wt.) were fed into barrel using a volumetric feeder KCV-KT20 (K-Tron, Niederlenz, Switzerland). Two feed rates were used, 2 and 4 kg/h, at a constant screw speed of 100 rpm. Fibers (20 wt. %) were fed manually after the matrix melting. The reason of manual fiber feeding is that no laboratory feeder is adapted for a homogeneous distribution of long natural fibers in polymer matrix, especially for very low feed rates (see mean and maximal fiber dimensions before processing in the Supplementary Data, Fig. S1). A special protocol with manual feeding was developed to ensure homogeneous fiber distribution in the compound (Supplementary Data, Fig. S2). It shows that no fiber content variation in samples could be a source of bias in this study. After steady-state was achieved, the extrudate was collected directly at the die exit, cut and analyzed with the methods described below.

Samples nomenclature is X-Y where X refers to fiber type (M for miscanthus and RH for retted hemp fibers) and Y to the feed rate (2 or 4 kg/h).

2.2.2 Matrix dissolution after compounding

For the scanning method, about 1 g of composite and 200 mL of Decalin[®] were placed in a round-bottom flask and stirred at 160 °C for 1.5 h at 400 rpm [8]. Before measuring fiber sizes, the suspension was diluted again with Decalin[®] in a proportion of 1:3 to avoid fibers overlapping.

For the automated method, composite samples were subjected to a reflux extraction method [11, 12] with p-xylene. The extracting system consisted of a round-bottom flask containing the solvent, a Knöpfler-Böhm extractor and a condenser. A thimble, made of a dedicated thick paper, retained the fibers. Then the fibers were dried in a vent hood for about 48 h.

It is well accepted in literature that solvents used to dissolve polymer matrix are not affecting natural fibers within experimental errors, and each dissolution method mentioned above is

widely used to determine fiber size distribution [8, 9, 20, 21]. In addition, control experiments were performed on hemp fibers alone submitted to the same reflux extraction method (data not shown). The mass recovery was found to be within 2% deviation.

2.2.3 X-ray microtomography

X-ray μ -CT image acquisition. A high resolution SkyScan 1174 X-ray μ -CT was used. The maximum peak voltage of the X-ray source is 50 kV with a maximum power of 40 W. The reflection target is made of tungsten and the focal spot is 50 μ m large. A 14-bit cooled CDD camera coupled to scintillator by lens with 1:6 zoom range sets up the detection system.

A cylindrical specimen of composite cut from the extrudate with the diameter (D_{spec}) of around 5 mm and the length (L_{spec}) of around 7 mm was glued to the top of the sample holder and placed between the X-ray source and the detector. The resolution achieved in these conditions is about 7 μ m. Projection images were taken every 0.5° rotation step over 360°. From this set of projection images the reconstruction of the 3D images was done by using a modified Feldkamp cone beam algorithm [22]. The whole image acquisition lasts almost 60 min with an exposure time of 1500 ms per projection. The whole image treatment, including the preparation of the sample, scan, reconstruction and data treatment lasts up to 5 h.

X-ray μ -CT image analysis. After 3D reconstruction, a region of interest is identified and selected. The segmentation is complicated by noise and systematic errors occurring during reconstruction. After a filtering step applied to suppress the noise, a resulting binary volume, containing the polymer matrix and the lignocellulosic material, is obtained using threshold operations. We checked that these methods (i.e. manual, maximum entropy, etc.) did not affect the final result.

The intensity-based segmentation cannot distinguish between the matrix surrounding the fibers and the lumen, i.e. the air enclosed inside a fiber, which is especially the case of porous miscanthus fibers. Thus a fiber “hole-filling” step was performed based on classical successive morphological operations [23]: a “closing” by reconstruction fills the lumen without modifying the fibers contours. The “hole-filling” procedure is extremely delicate because it may affect the

estimation of the fiber diameter, which is realized here through openings by a structuring element with growing size (openings is the first method described in “X-ray μ -CT granulometry method” section) [24, 25].

In a second method (see “X-ray μ -CT method of estimation of fiber length and diameter” section) used to evaluate both length and diameter, each fiber had to be identified after hole-filling and labeled. Figure 1 shows the 3D reconstruction of the volume in which, to make easier the visualization, one label/fiber corresponds to one color.

In both methods the particles and the fibers touching the upper and the lower edges of the examined cylindrical volume were not taken into account.

X-ray μ -CT granulometry method: principle of estimation of fiber diameter. Once segmented and binarized, 3D images were obtained and fiber size analysis was performed. The principle of building size distribution is to apply successive openings with structuring elements of increasing size on the tested volume [26]. Performing an opening reproduces the mechanism of sieving: particles of the size smaller than a structural object of a given geometrical form (for example, a cube, a sphere, or an octahedron) and a given size are removed. The opening operation ends when there are no more fibers in the volume [27]. The structuring element in this work is an octahedron of size λ and diameter d ; it is the biggest element that can be inscribed within the fiber/bundle (see for more details Fig. S3 in Supplementary Data). The resolution multiplied by d provides the diameter of the fiber, D , expressed in μm . In this study the smallest D that can be estimated is $14 \mu\text{m}$. For each opening, the normalized cumulated size distribution (NG) of the fibers the diameter of which is smaller than d is calculated as follows [24]:

$$NG(\lambda) = 1 - \frac{V_\lambda}{V_o} \quad (1)$$

where V_o and V_λ are the sum of voxels occupied by fibrous phase in the original image and in the volume opened by the λ -th octahedron, respectively. The granulometry density function of fibers with one certain diameter is obtained by the difference between two successive cumulated diameter fractions:

$$G(\lambda) = NG(\lambda + 1) - NG(\lambda) \quad (2)$$

Further details about the method used can be found in the paper of Hamdi et al. [6]. The interpretation of D depends on the cross-sectional shape of the fibers: if the cross-section is circular or elliptical, D is related to the diameter or the minor axis, respectively.

X-ray μ -CT method of estimation of fiber length and diameter. With the opening method described above, only fiber diameter D can be estimated. In order to obtain both length, L , and diameter, it is necessary to identify each fiber individually (Fig. 1) and to use various approximations. To do this, the 3D Object Counter Plugin of ImageJ, a Java image processing program, is used [28].

In a first step, each fiber was inscribed into a parallelepiped the height, width and depth of which were provided by the software (Fig. 1A). From the visual observation of the fibers in the 3D images, it was assumed, in the first approximation, that the majority were straight and cylindrical with uniform and circular section. Then their length was estimated as a diagonal line of the parallelepiped (red line in Fig. 1A) by applying the Pythagoras theorem. In the rest of the manuscript, we refer to the results obtained in this way as “Pythagoras” approximation. This approximation clearly leads to an underestimation of L when fibers are bent and curved (see Fig. 1B).

In the second approximation (named “ V/S ”), we assumed that the fibers were cylindrical and may twist. The whole surface (S) and the volume (V) values in pixels were provided by the software. Considering that V is equal to $\pi D^2 L/4$ and S could be approximated by the lateral surface $S_{lat} = \pi D L$, L can be estimated as the ratio $S_{lat}^2/(4\pi V)$. With this approximation, contrarily to the “Pythagoras” one, the length of long fibers is overestimated. Finally, assuming that the fibers are straight, as mentioned above, and more or less parallel to sample main axis (Fig. 1), fibers longer than 7000 μm (length of the sample) were ignored.

In both approximations, the equivalent diameter of the fiber was calculated as $4V/S_{lat}$.

2.2.4 2D high-resolution image scanning

Image acquisition. The diluted suspension was poured on a glass slide (see Fig. S4 in Supplementary Data), covered and mounted on the scanner. 8-bits greyscale images in an

uncompressed format were acquired with an Epson Perfection™ V550 Photo Color Scanner, in transmission mode and with a resolution of 6400 dpi, corresponding to 4 μm/pixel (Fig. S4a).

Image processing, segmentation and analysis. The image analysis was carried out by employing ImageJ. The segmentation of the images was achieved manually by applying a fixed grey level threshold value on the image; several image parts were controlled to ensure that no fiber was missed during the process. Particles were labeled thanks to the plugin “Morphology > BinaryLabel8” developed by Landini [29] that resulted in a new 16 bit greyscale image with re-scaled brightness (Fig. S4b). Once the labeled image was created, the plugin “Geodesics > Geodesics Diameters” [30] was applied to compute the fiber size by quantifying the geodesic distance map in the binary image. Distances were determined using the Borgefors (3,4) algorithm [31] (i.e. chamfer weights), which yields a good compromise between precision and rapidity [19]. For each fiber/label, the algorithm assessed the radius of the circle inscribed within the fiber (geodesic length) and the aspect ratio, L/D (geodesic elongation).

2.2.5 Automated fiber analysis

The third methodology employed to assess fiber size distribution is a MorFi Compact® fiber analyzer (Techpap SAS, Grenoble, France). The analysis was performed in a dynamic mode on a suspension of fibers dispersed in water flowing through the cell. A camera with a resolution of 1280 × 960 pixels and an accuracy of 11.5 μm/pixel (i.e. a window of 14.72 mm × 11.04 mm), recorded the fibers images. Fibers touching the observation window were not taken into account; hence, all the elements longer than approximately 10 mm were excluded from the analysis. The longer the fiber, the higher is the probability that it touches the window: a 5600 μm long fiber has 50% of probability of touching, while for a 10000 μm long fiber the probability is higher than 80%. Moreover, when the regular analysis mode is used as herein, elements shorter in length than 100 μm were neglected by the analysis software.

Figure 2 summarizes the different phases in sample preparation for the analysis of fiber sizes required by each method. In all cases, the number of analyzed fibers was around 2000 and

higher (with the exception of the M-2 sample where the number of elements was 1143), ensuring a statistical significance.

2.3 Analysis of fiber size distribution

The frequency distribution of a data set is an important factor determining the type of statistical analysis that can be carried out. Numerous statistical methods require normally distributed data (e.g. Gaussian distribution). However, many measurements, such as the size distribution of fibers in a composite, show more or less skewed distributions, described by log-normal [32] or two-parameters Weibull laws [9, 31]. We employed the log-normal probability density function, $f(x)$, given by the following equation:

$$f(x) = \frac{1}{x\sigma\sqrt{2\pi}} \exp\left[-\frac{1}{2}\left(\frac{\ln x - \mu}{\sigma}\right)^2\right] \quad (3)$$

where μ is the mean value (or “location parameter”), σ is the standard deviation (or “shape parameter”) of the logarithm of the variable x , being here either fiber length L , or diameter D , or aspect ratio L/D . A two parameter Weibull distribution $f(x)$ was also tested, but the goodness-of-fit was higher for log-normal distribution than those for Weibull distribution.

A non-parametric method was also used for comparison: it is represented by the box-and-whiskers plot, which is an immediate and compact way to graphically display at one glance the spread of all the experimental data points in one plot [9]. Figure 3 shows an example of the frequency distribution calculated from the log-normal law $f(x)$ (Fig. 3a) and the box-and-whiskers representation (Fig. 3b), for M-2 sample diameter data. The vertical full line in the box plot depicts the median (Q_2) and dashed lines correspond to the lower (Q_1) and the upper (Q_3) quartiles and to the lower (D_1) and the upper (D_2) deciles. The cross and the circle depict the number average and the weighted average values, respectively. The data shown are concentrated on low diameter values: the distribution is skewed right or positively skewed.

We also calculated the average values weighted in number [8] (also sometimes called as arithmetic mean [18] or number average [17]), L_n , D_n and $(L/D)_n$, and the average values

weighted in weight [8] (or "contraharmonic mean", also called as weight average [6, 17]), L_w , D_w and $(L/D)_w$ [17]:

$$x_n = \frac{\sum_{i=1}^N n_i x_i}{\sum_{i=1}^N n_i} \text{ and } x_w = \frac{\sum_{i=1}^N n_i x_i^2}{\sum_{i=1}^N n_i x_i} \quad (4)$$

where x_i is the fiber size in class i , n_i is the corresponding number of fibers, and N is the total number of fibers. When the size of each fiber is known, Eq. (4) becomes $x_n = \sum_{i=1}^N x_i / N$ and $x_w = \sum_{i=1}^N x_i^2 / \sum_{i=1}^N x_i$, respectively. The number average is strongly affected by a large number of small entities, while the weight average emphasizes the presence of long ones.

3. RESULTS AND DISCUSSION

3.1. Fiber sizes obtained with different methods

Each method employed to assess fiber dimensions has technical restrictions in size resolution, summarized in Fig. 4. The limitations in fiber length are not always the same as for fiber diameter within the same method. The minimum fiber length, below which it cannot be measured, is 4 μm for 2D scanner, 60 μm for $\mu\text{-CT}$ (for both "Pythagoras" and "V/S" approximations) and theoretically (optical detection) 5 μm for the automated analyzer MorFi[®] which in practice is about 100 μm due to image analysis settings. For diameter the minimum size is 4 μm for 2D scanner, 5 μm for MorFi[®] and 14 and 20 μm for $\mu\text{-CT}$ granulometry and "Pythagoras"- "V/S" approximations, respectively. As for the maximal length values, scanner does not have any particular limitations, $\mu\text{-CT}$ is restricted by sample size (L_{spec} and D_{spec}) and MorFi[®] by the size of the visualization window, i.e. a maximal length of 10 000 μm . For the maximal diameter, no particular limitation is imposed by the measuring methods used, but it seems that diameter larger than 160 μm cannot be measured with MorFi[®]. The reason is the limitation of MorFi[®] for measuring long fibers (see Section 2.2.5), and the fact that long fibers are usually thick bundles. Thus, indirectly, both long and thick fibers are excluded from the analysis by MorFi[®]. In all methods, except the granulometry, a pair of length and diameter values is associated to each fiber.

To illustrate the influence of size limitations of each method on fiber size distribution, log-normal distributions of fiber length, diameter and aspect ratio for RH-2 sample were plotted in Fig. 5. Distribution parameters, μ and σ , were calculated for all composites (Table 1). The length distributions obtained with different methods for RH-2 are all asymmetrical and with a positively skewed shape (Fig. 5a). σ_L values are very close to 1, ranging between 0.722 and 1.093. However, any further comparison becomes arduous because of different size intervals imposed by the measuring method. The prominence of small particles (between 4 and 60 μm that can be assessed by 2D scanner) on the length distribution is reflected by $\sigma_L > 1$ for the all fibers studied (Table 1), and low mean value, i.e. $\mu_L = 3.730$. μ_L reached a value of 4.753 if only particles longer than 60 μm were considered, and values from 5.343 to 5.905 if the measure is restricted to fibers longer than 100 μm .

Table 2 shows how mean values, in particular number average, are strongly influenced if small particles were considered (case of 2D scanner) or not (cases of MorFi[®] and μ -CT tomography, “Pythagoras” and “V/S” approximations). For the case of RH-2 sample the largest L_n was obtained with MorFi[®] method (519 μm), followed by μ -CT (342 μm for “V/S” and 167 μm for “Pythagoras”) and then by 2D scanner (100 μm). Weight-averaged values emphasize large sizes; thus, L_w values obtained with 2D scanner and MorFi[®] analyzer are closer, 806 and 939 μm , respectively (Table 2). “Pythagoras” approximation seems to strongly underestimate L_w (462 μm), while “V/S” overestimates it (1257 μm). D_n and D_w values are rather similar (Table 2).

In order to understand if the reason of the differences in size distributions (Fig. 5a) is only due to the interval of sizes considered, we applied to all data a threshold L_{thres} of 100 μm , which is the minimum length value assessed by MorFi[®] method (Fig. 5b). Length distributions showed a tendency to superimpose and μ_L (ranging from 5.343 to 5.905) and σ_L (from 0.812 to 0.833) parameters had similar values (Table 1), with the exception of $\sigma_L = 0.690$ evaluated by “Pythagoras” approximation, that was slightly lower than the others. The distributions and their parameters were even closer if a larger threshold, $L_{thres} = 200 \mu\text{m}$, was used (Fig. S5 and Table

1). The shape of the length distributions of M-4 and RH-2 samples, both investigated by 2D scanner, was strongly affected depending if all elements were counted in the analysis or if only fibers larger than a certain threshold, L_{thres} , were taken into account (Fig. S6 in Supplementary Data). We can thus conclude that for the same fibers the interval of sizes imposed by the measuring method strongly determines fiber size distribution and mean values. This result is expected from statistical approach.

Contrary to fiber length, diameter distributions exhibited the biggest dissimilarity. As L_{thres} was applied, D distributions shifted towards larger values (from 2.982 to 3.860 for 2D scanner), as expected, but no superposition occurred (Fig. 5b). 2D scanner results showed larger μ_D than MorFi[®] (3.450) and μ -CT (3.396–3.582). The μ -CT data were characterized by intermediate μ_D and very low σ_D (0.194-0.219), reflecting a more symmetrical shape (Table 1).

The methods used gave comparable length if small elements (shorter than 100 μm) were ignored. The differences between the diameter distributions even after the threshold applied (σ_D varies from 0.2 for μ -CT data to 0.6 for MorFi[®], μ_D from 3.4 for μ -CT to 3.9 for 2D scanner) suggest that the interval of sizes imposed by the measuring method is not the only parameter affecting size distribution results.

3.2 Diameter distributions: comparison of methods

The comparison between diameter sizes obtained with different methods will be now performed by using box-and-whiskers plots (Figs. 6-8) and log-normal distribution parameters. In this presentation the bisector means that the values obtained with different methods coincide.

3.2.1 2D scanner vs. Automated analyzer

First, the results obtained by 2D scanner and MorFi[®] analyzer were compared for L_{thres} equal to 100 and 200 μm . For miscanthus fibers (M-4, Fig. 6a and RH-2, Fig. 6b), diameter data obtained by both methods were in agreement for lower deciles, quartiles and median values; but the upper D_2 and Q_3 values assessed by 2D scanner were by a factor of 2 higher than the values obtained by MorFi[®] analyzer, which do not allow measurement of diameters larger than 160 μm . Such important departure from bisector was not observed for hemp fibers (RH-2, Fig. 6b)

that are, in general, thinner than miscanthus fibers, although for the 2D scanner RH data were larger (by about 30%) than those measured by the automated analyzer.

3.2.2 μ -CT granulometry vs. Automated analyzer and 2D scanner

Table 2 shows that mean values of the diameter assessed by granulometry are closer to D_w values calculated from 2D scanner and MorFi[®] analyzer than D_n values. In general, D values of μ -CT granulometry are slightly larger than those estimated by MorFi[®] method and lower than those measured by 2D scanner. For hemp samples (RH-2 and RH-4, Fig. 7a and b, respectively), lower deciles, quartiles and median values coincide for all three methods but some difference can be seen for RH-4 for higher deciles and quartile between μ -CT granulometry and 2D scanner. For the miscanthus, a similar trend was observed: the difference between diameter values obtained with different methods appears at higher deciles and quartiles values: 2D scanner shows higher values and MorFi[®] lower values than μ -CT (Fig. 7 c-d).

Figure 8 shows the comparison between diameter values obtained with granulometry and all the other approaches, i.e. 2D scanner, MorFi[®] analyzer, and μ -CT ("Pythagoras" and "V/S" approximations), for RH-2 fibers. Diameter size distribution obtained with granulometry has similar properties as those obtained with 2D scanner and MorFi[®] analyzer, but there are some divergences from the distribution evaluated by "Pythagoras" and "V/S" approximations. All differences again occur at higher deciles and quartiles values: granulometry median (Q_2) and upper percentiles (Q_3 and D_2) were overestimated with respect to these evaluated by both "Pythagoras" and "V/S" approximations (Q_2 by a factor of 1.2, Q_3 of 1.5, and D_2 of 2.0). On the contrary, lower percentiles, D_1 and Q_1 , were underestimated. The shape of the granulometry distribution is, therefore, more asymmetric than that determined by "Pythagoras" and "V/S" approximations (Fig. 5 and Fig. 8).

3.3. Pros and cons of each method

Two types of fibers of different phenotypes and morphologies (hemp with thinner bundles made of small lumen size elementary fibers; miscanthus with large and porous bundles) were used in this study to demonstrate the problems that can occur during the analysis of their

dimensions with various methods. The results obtained show that fiber size distribution may be affected by several factors, such as the experimental method employed (see advantages and disadvantages in Table 3), the choice of the variables describing the size analysis, and also by the way samples are prepared.

In terms of sample preparation, X-ray μ -CT tomography does not require any specific treatments while 2D scanner and MorFi[®] methods need fiber separation from the polymer. The accuracy of 2D scanner, which is nominally equal to the half of the imposed resolution (in this work $\pm 2 \mu\text{m}$), strongly depends on suspension transparency as far as imperfections contribute to noise increase and thus to systematic errors. It is, therefore, “user-dependent”, but it does not have any restrictions on fiber sizes except very small ones below $4 \mu\text{m}$. The advantage of MorFi[®] vs 2D scanner is that the former is automatic which excludes “personal” factor in sample preparation. At the same time, MorFi[®] has intrinsic limitations in measured sizes, both technical as well as due to its software (Table 3).

For μ -CT, image processing and segmentation are very complex, especially in the case of large lumen in fibers or bundles, like in miscanthus, requiring an accurate fiber hole-filling step. Fiber labeling involves a delicate work of image interpretation (Fig. 1): a bended fiber is certainly a single fiber (case B), two contiguous fibers could pass for one bended fiber (case C), a very long fiber can actually be the sequence of three aligned fibers (case D), or a bundle could be taken for two close fibers (case E). It is clear, therefore, that the presence of ambiguous cases and their erroneous evaluation could affect the size analysis. μ -CT is thus “user-dependent”. In particular, in “Pythagoras” approximation, each labeled fiber was considered straight; hence, when a bended element was encountered (as fiber A in Fig. 1), the apparent length, approximated to the parallelepiped diagonal, is shorter than the real length. This approach leads, therefore, to the underestimation of L with respect to “ V/S ” approximation, resulting in larger μ_L and smaller σ_L (Table 1) and lower L_n and L_w (Table 2) as L_{thres} is increased.

The comparison of fiber length distributions (Fig. 5) shows that they mainly depend if the method used has any restrictions towards the interval of length values. When using the same

interval of sizes for each method, length distributions are very similar, which follows from basic statistical approach. The restrictions in length values, as imposed in MorFi[®], considerably restrain the length limits: fibers and particles shorter than 100 μm are neglected (sometimes even shorter than 200 μm [12]), which leads to a strong distortion in fiber size distributions. The situation is more complex with the analysis of diameter distributions assessed by different methods. 2D scanner may have a tendency to overestimate D values. The reason is that elementary fibers and bundles are usually flat, i.e. having elliptical cross-section (Fig. S1). When fiber suspension is poured on the glass, fibers lay down on their major axis due to gravitational force. Thus, scan observations measure the largest diameter (Fig. S7). The diameters measured by MorFi[®] are the smallest (Figs. 5b, 6 and 7). This is because fibers which length is comparable with visualization window size are excluded from the analysis (Fig. 4). Longer fibers are usually also the thickest; hence, if long elements are not taken into account, an underestimation of the diameter may occur (Figs. 6 and 7). The fact that MorFi[®] analyzer did not count any fiber thicker than 160 μm (Table 2) may be caused by this constraint. This limit was more pronounced for miscanthus the fibers of which are longer and thicker than those of hemp. In order to improve the morphology analysis by MorFi[®], a modification of the visualization technique, i.e. the dimension of the camera window, should be considered.

The precision of X-ray μ -CT tomography is strictly linked to sample dimensions; it is recommended, therefore, to analyze small specimens to achieve high resolution, as it has been pointed out by Miettinen et al. [5]. The plausible loss of information about large elements that could touch sample edges may explain the differences between 2D scanner and automated μ -CT tomography values (Fig. 7). Moreover, granulometry was related to the minor axis of the fiber cross-section. The principle of the openings approach (paragraph 2.2.3) is, in fact, based on that fact that the diameter is associated to the size of the largest structural element inscribed in the fiber (Fig. S3 and D_{min} in Fig. S7), whilst 2D scans were related to its major axis (Fig. S7). Finally, the underestimation of L produced by “Pythagoras” approximation made sure that a larger number of small and thin fibers, with respect to “ V/S ” approximation, is not taken into

account when L_{thres} is applied. As a consequence, diameter values, estimated by “Pythagoras” approximation, are slightly larger than those by “V/S” one (Fig. 8, Table 2).

6. CONCLUSIONS

Three methods, 2D scanner, automated analyzer MorFi[®] and microtomography were used to analyze natural fiber length and diameter distributions in the same composites. We showed that the analysis of lignocellulosic fibers’ dimensions is still complex and does not allow, for the time being, an un-biased estimation of fiber sizes. Each method has its advantages and disadvantages. The advantage of 2D scanner is that it does not have any restrictions on fiber sizes except very small ones below a few microns; however, it requires polymer dissolution and is not “user-independent”. The advantage of MorFi[®] analyzer and the family of similar analyzers is that it is automatic, but it also requires polymer dissolution. MorFi[®] has intrinsic limitations in measured sizes, both technical as well as of its software. X-ray μ -CT tomography is a 3D non-invasive *in situ* method. Its main drawbacks are that it needs high cost investments and the resolution depends on the sample’s dimensions. Overall, the three methods are complementary and the use of each depends on the goal of the work.

ACKNOWLEDGEMENTS

This work was supported by National French Agency for Research (ANR), through the “DEFIBREX” project (ANR-12-RMNP-0004). The team from Reims was also supported by the Competitiveness Cluster Industries & Agro-Resources (IAR). The team from Bordeaux thanks ANR for supporting this study through the XYLOMAT project “XYLOFOREST” (ANR-10-EQPX-16). FRD[®] company (Troyes, France) is gratefully acknowledged for providing the fibers.

REFERENCES

- [1] Mohanty A, Misra M, Drzal L. Sustainable bio-composites from renewable resources: Opportunities and challenges in the green materials world. *J Polym Environm* 2002;10:19-26.

- [2] Joshi S, Drzal L, Mohanty A, Arora S. Are natural fiber composites environmentally superior to glass fiber reinforced composites? *Composites: Part A* 2003;35:371-376.
- [3] Faessel M, Delisée C, Bos F, Castéra P. 3D Modelling of random cellulosic fibrous networks based on X-ray tomography and image analysis. *Compos Sci Tech* 2005;65: 1931-40.
- [4] Alemdar A, Zhang H, Sain M, Cescutti G, Müssig J. Determination of fiber size distributions of injected moulded polypropylene/natural fibers using X-ray microtomography. *Adv Engin Mat* 2008; 10:126-130.
- [5] Miettinen A, Luengo Hendriks C, Chinga-Carrasco G, Gamstedt E, Kataja M. A non-destructive X-ray microtomography approach for measuring fibre length in short-fibre composites. *Compos Sci Technol* 2012; 72:1901-08.
- [6] Hamdi S, Delisée C, Malvestio J, Le Duc A, Da Silva N, Beaugrand J. X-ray computed microtomography and 2D image analysis for morphological characterization of short lignocellulosic fibers raw materials: A benchmark survey. *Composites: Part A* 2015;76:1-9
- [7] Terenzi A, Kenny J, Barbosa S. Natural fiber suspensions in thermoplastic polymers. I. Analysis of fiber damage during processing. *J Appl Polym Sci* 2007;103:2501-06.
- [8] Le Duc A, Vergnes B, Budtova T. Polypropylene/natural fibres composites: Analysis of fibre dimensions after compounding and observations of fibre rupture by rheo-optics, *Composites: Part A* 2011;42:1727-37.
- [9] Le Moigne N, van den Oever MJA, Budtova T. A statistical analysis of fibre size and shape distribution after compounding in composites reinforced by natural fibres. *Composites: Part A* 2011;42:1542-50.
- [10] Gonzalez-Sanchez C, Gonzalez-Quesada M. Novel automated method for evaluating the morphological changes of cellulose fibres during extrusion-compounding of plastic-matrix composites. *Composites: Part A* 2015;69:1-9.
- [11] Beaugrand J, Berzin F. Lignocellulosic fiber reinforced composites: influence of compounding conditions on defibrization and mechanical properties. *J Appl Polym Sci* 2013;128:1227-38.
- [12] Berzin F, Vergnes B, Beaugrand J. Evolution of lignocellulosic fibre lengths along the screw profile during twin screw compounding with polycaprolactone. *Composites: Part A* 2014;59:30-36.
- [13] Chinga-Carrasco G, Solhein O, Lenes M, Larsen A. A method for estimating the fibre length in fibre-PLA composite. *J Microscopy* 2013;250:15-20.
- [14] Reme P, Johnsen P, Helle T. Assessment of fibre transverse dimensions using SEM and image analysis. *J Pulp Pap Sci* 2002;28:122-128.
- [15] John M, Anandjiwala R. Recent developments in chemical modification and characterization of natural fiber-reinforced composites. *Polym Compos* 2008;29:187-207.

- [16] Herrera-Franco P, Valadez-Gonzalez A. A study of the mechanical properties of short natural-fiber reinforced composites. *Composites: Part B* 2005;36:597-608.
- [17] Yilmazer U, Cansever M. Effects of processing conditions on the fiber length distribution and mechanical properties of glass fiber reinforced nylon-6. *Polym Compos* 2002;23:61-71.
- [18] Quijano-Solis C, Yan N, Zhang S. Effects of mixing conditions and initial fiber morphology on fiber dimensions after processing. *Composites: Part A* 2009;40:351-358.
- [19] Legland D, Beaugrand J. Automated clustering of lignocellulosic fibres based on morphometric features and using clustering of variables. *Indus Crops Prod* 2013;45:253-261.
- [20] Bos HL, Müssig J, van den Oever MJA. Mechanical properties of short-flax-fibre reinforced compounds. *Composites: Part A* 2006;37:1591-1604.
- [21] Ganster J, Fink HP. Novel cellulose fibre reinforced thermoplastic materials. *Cellulose* 2006;13:271-280.
- [22] Feldkamp L, Davis L, Kress J. Practical cone beam algorithm. *J Microscopy* 1997;185:67-75.
- [23] Walther T, Terzic K, Donath T, Meine H, Beckmann F, Thoemen H. Microstructural analysis of lignocellulosic fiber networks. *Proceedings of Conference on Developments in X-ray Tomography V*, SPIE Volume 6318, 2006 San Diego, California.
- [24] Matheron G. (1967). *Éléments pour une théorie des milieux poreux*, Paris, Masson.
- [25] Serra J. (1988). *Image Analysis and Mathematical Morphology: Theoretical Advances*. Vol. 2, Academic Press, London.
- [26] Dougherty E R. Granulometric size density for segmented random-disk models. *J Math Imag Vision* 2002;17:271-281.
- [27] Dougherty E R, Cuciurean-Zapan C. Optimal reconstructive τ -openings for disjoint and statistically modeled nondisjoint grains. *Signal Proc* 1997;56:45-58.
- [28] Bolte S, Cordelières F. P. A guided tour into subcellular colocalization analysis in light microscopy, *Journal of Microscopy* 2006;224:213-232.
- [29] www.mecourse/landinig/software/software.html
- [30] <http://www.pfl-cepia.inra.fr/index.php?page=geodesic-diameter>
- [31] Borgefors G. Distance transformations in digital images. *J Comput Vision Graph Image Proc* 1986;34:344-371.
- [32] Jiang B, Liu C, Zhang C, Wang B, Wang Z. The effect of nonsymmetric distribution of fiber orientation and aspect ratio on elastic properties of composites. *Composites: Part B* 2007;38:24-34.
- [33] Aykol M, Isitman N, Firlar E, Kaynak C. Strength of short fiber reinforced polymers: Effect of fiber length distribution. *Polym Compos* 2008;29:644-648.

FIGURE CAPTIONS

Figure 1. 3D reconstructed volume visualization of segmented and labeled hemp fibers (RH-2). Insets describe A) the Pythagoras approximation; and particular cases as B) a curved fiber; C) a bended long fiber or two close fibers; D) a very long fiber; E) two separated elementary fibers or a bundle. Each fiber is correlated to one color; more than 3000 colors have been used. Human eye cannot distinguish very similar colors, but the software provides all data.

Figure 2. Outline of the steps required by each method to assess fibers' dimensions.

Figure 3. Representation of a) the frequency diameter distribution and b) the box-plot for the M-2 composite. Deciles (lower: D_1 and higher: D_2), percentiles (lower: Q_1 and higher: Q_2), number average and weight average are displayed.

Figure 4. Scheme describing the window of sizes that can be assessed by each method. The maximal limit of 2D scanner methodology is given by the dimensions of the scanner window.

Figure 5. Probability density function for length, diameter and aspect ratio distributions for RH-2 data with a) no threshold applied to fiber length; b) with $L_{thres} = 100 \mu\text{m}$

Figure 6. Upper and lower deciles (squares), upper and lower quartiles (circles), and median (triangles) plotted for M-4 (a) and RH-2 (b) diameters analyzed by MorFi[®] analyzer (x -axis) and 2D scanner (y -axis). Filled and open symbols designate the threshold $L_{thres} = 100 \mu\text{m}$ and $200 \mu\text{m}$, respectively. Black line depicts the bisector $x = y$.

Figure 7. Upper and lower deciles (squares), upper and lower quartiles (circles), and median (triangles) plotted for a) RH-2, b) RH-4, c) M-2, and d) M-4 diameters. Data obtained by 2D scanner (filled symbols) and by MorFi[®] (open symbols) were plotted on y -axis ($L_{thres} = 100 \mu\text{m}$), granulometry by μ -CT on x -axis (resolution of $14 \mu\text{m}$).

Figure 8. Comparison of the diameters obtained with granulometry data (x -axis) with all other analysis methods (y -axis) for RH-2 samples. D and Q indicate deciles and quartiles, respectively, the subscript numbers are as in Figure 3a.

Supplementary Data

Reliability evaluation of automated analysis, 2D scanner and micro- tomography methods for measuring fiber dimensions in polymer- lignocellulosic fiber composites

E. Di Giuseppe, R. Castellani, S. Dobosz, J. Malvestio, F. Berzin, J. Beaugrand, C.

Delisée, B. Vergnes, T. Budtova

Figure S1.

SEM image of hemp fibers a) before compounding, and c) in the composite; miscanthus fibers b) before compounding, and d) in the composite.

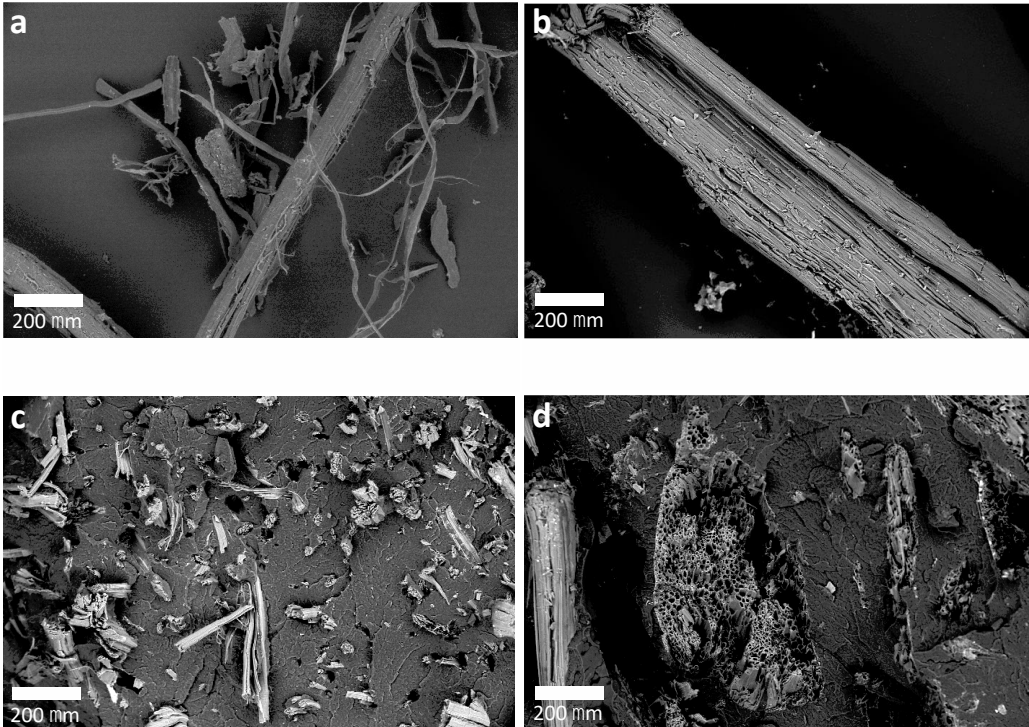
The initial mean and maximal sizes are also indicated for each case

HEMP

$L_n = 302 \text{ mm}$, $D_n = 37 \text{ mm}$, $(L/D)_n = 4.5$
 $L_w = 2517 \text{ mm}$, $D_w = 100 \text{ mm}$, $(L/D)_w = 17.6$
 $L_{max} = 13100 \text{ mm}$, $D_{max} = 1937 \text{ mm}$

MISCANTHUS

$L_n = 245 \text{ mm}$, $D_n = 67 \text{ mm}$, $(L/D)_n = 2.1$
 $L_w = 1910 \text{ mm}$, $D_w = 240 \text{ mm}$, $(L/D)_w = 4.3$
 $L_{max} = 8860 \text{ mm}$, $D_{max} = 1093 \text{ mm}$



The SEM transversal images of a bundle in Figure S1d shows that miscanthus fibers have a large lumen that makes the fibers highly porous compared to hemp fibers (Figure S1c). The dimensions of the fibers before compounding have been assessed by 2D scanner.

Table S1

Screw profile (from hopper to die).

Temp. (°C)	60	180	180	180	180	180	180	180	180	180	180	180	180	180
Length (mm)	200	25	25	25	150	50	75	25	100	25	75	25	50	50
Pitch (mm)	33	25	16	25 Left	33	25	16	KB* 90/5	25	25	16	KB* -45/5	25	16

* KB -45/5 means kneading discs block of 5 elements, with a staggering angle of -45° (left-handed).

The screw profile, composed of two-flighted conveying screw elements of various pitches, and two mixing zones (block of five kneading discs), is depicted in Table S1. The barrel is regulated at a fixed temperature (60°C for first barrel, 180°C for the others). Two feed rates were used, 2 and 4 kg/h, both at a constant screw speed of 100 rpm.

Because the initial fibers were long (see Figure S1 with fibers' number and weight average values and maximal values), a special procedure of manual feeding was developed. It prevents irregular feeding and thus heterogeneous fiber distribution in the compound that usually happens when long lignocellulosic fibers are fed with either volumetric or gravimetric feeders. To do so, for instance, if the final feed rate was 2 kg/h, the throughput was 1.6 kg/h for polymer and 0.4 kg/h for fibers (and for 4 kg/h, 3.2 kg/h and 0.8 kg/h). The regularity and the accuracy of the fiber feed rate was controlled by regularly weighing the output of the composite.

The illustration of the homogeneous distribution of fibers in the composites is demonstrated in Figure S2.

Figure S2

Illustration of sampling of extrudate strands for the determination of fiber content in composites and the corresponding fiber content.

Because the regularity of the feeding is of major importance, one operator was especially devoted to feed by hand the fibers in the extruder. First, 400 sets (or “aliquots”) of 2 g of dry fibers each were prepared before compounding. Then, each aliquot was fed in three times within a strict interval of 9 seconds. After cooling down the extrudates to room temperature, 12 samples of approximately 2 g of composite were cut from extrudates at every 10 cm (Figure S2). The samples were subjected to a reflux extraction method with p-xylene. After matrix dissolution, the fibres were collected, dried, weighted and their mass content in the composite calculated. The concentration of fibers in all twelve samples is shown in Figure S2. The average value satisfied 20 ± 2 wt.% target (see shadow area in Figure S2).

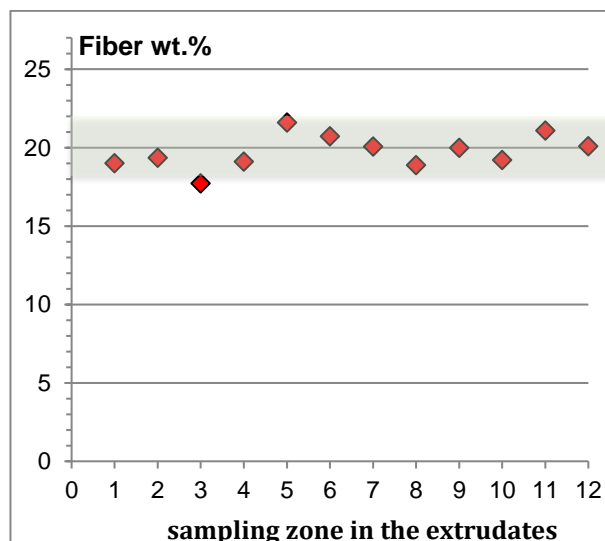
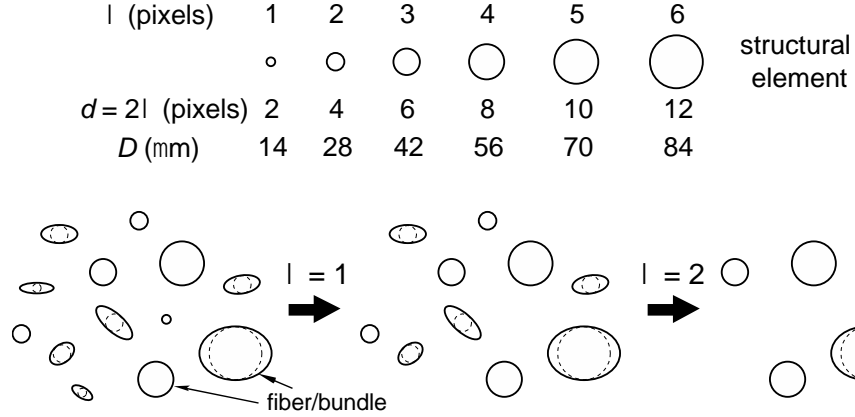


Figure S3

Opening operation with structural elements: a schematic illustration of the structural elements of increasing size, λ , applied on the tested volume and the opening technique for $\lambda = 1$ and $\lambda = 2$. The structural element is the biggest element that can be inscribed within the fiber/bundle (dashed circles).



The diameter d of the structural element of size λ is given by 2λ and measured in pixel units. The normalized cumulated size distribution, NG , of the fibers whose diameter is smaller than $(2\lambda + 1)$ is calculated as follows [24]:

$$NG(\lambda) = 1 - \frac{V_\lambda}{V_0} = P_r\{D < d = (2\lambda + 1)\} \quad (\text{S3.1})$$

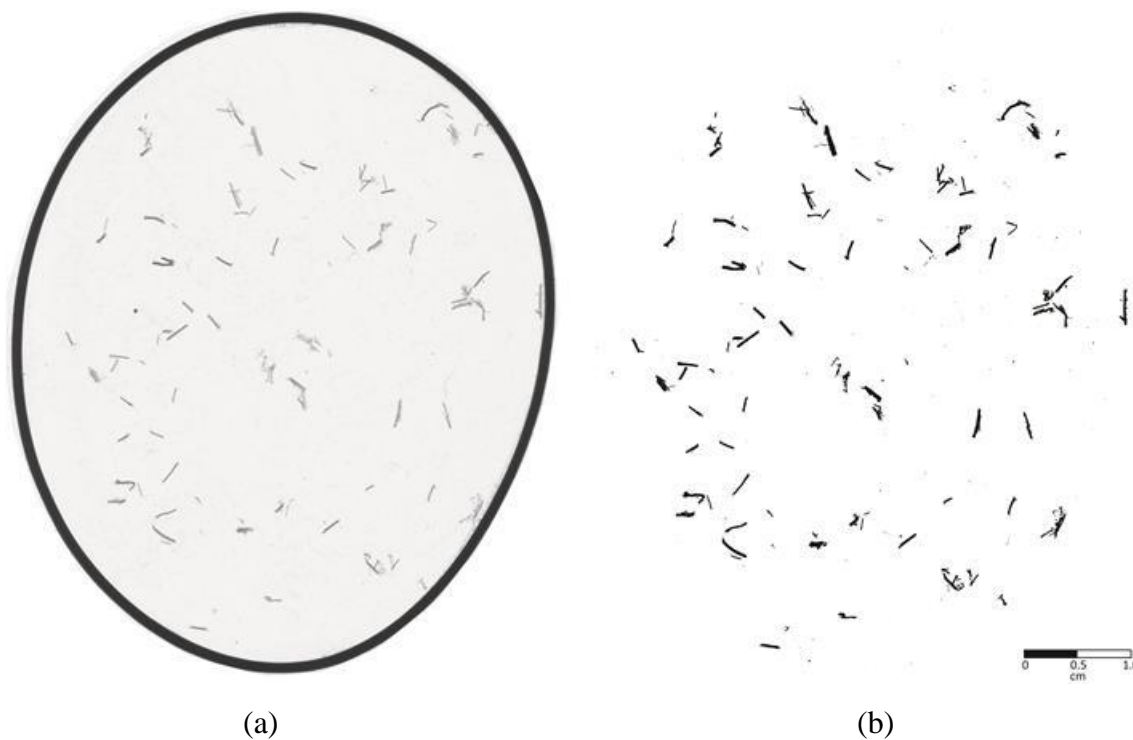
In particular, the size distribution of the fiber diameter D is obtained as:

$$NG(\lambda) = 1 - \frac{V_\lambda}{V_0} = P_r\{D < d = 2\lambda\} \quad (\text{S3.2})$$

The resolution achieved by the system is $7 \mu\text{m}$, hence, fiber diameter, D , is calculated as $d \times \text{resolution}$.

Figure S4

2D image scanning and segmentation: image of the fiber/Decalin[®] suspension a) inside the joint and b) the segmented image



A volume of approximately 0.2 mL of suspension was deposited on a rectangular glass slide ($100 \times 200 \times 2 \text{ mm}^3$) within the area limited by an elastomeric joint (diameter around 50 mm, with a cross-section of diameter 1 mm) glued to the glass to limit fluid spreading. The suspension, once poured, was covered (to avoid solvent evaporation) with a second glass slide and all mounted on the scanner. Before proceeding with the segmentation, the images had to be cropped to remove the joint and what is beyond it.

Figure S5

Influence of threshold length $L_{thres} = 200 \mu\text{m}$ on size distributions. Probability density function for length, diameter and aspect ratio distributions for RH-2 data with $L > 200 \mu\text{m}$.

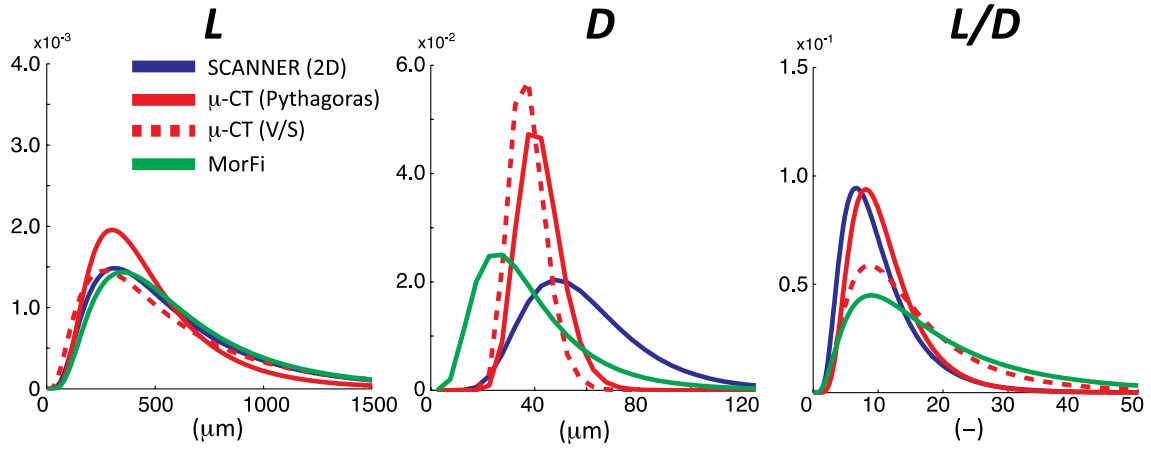
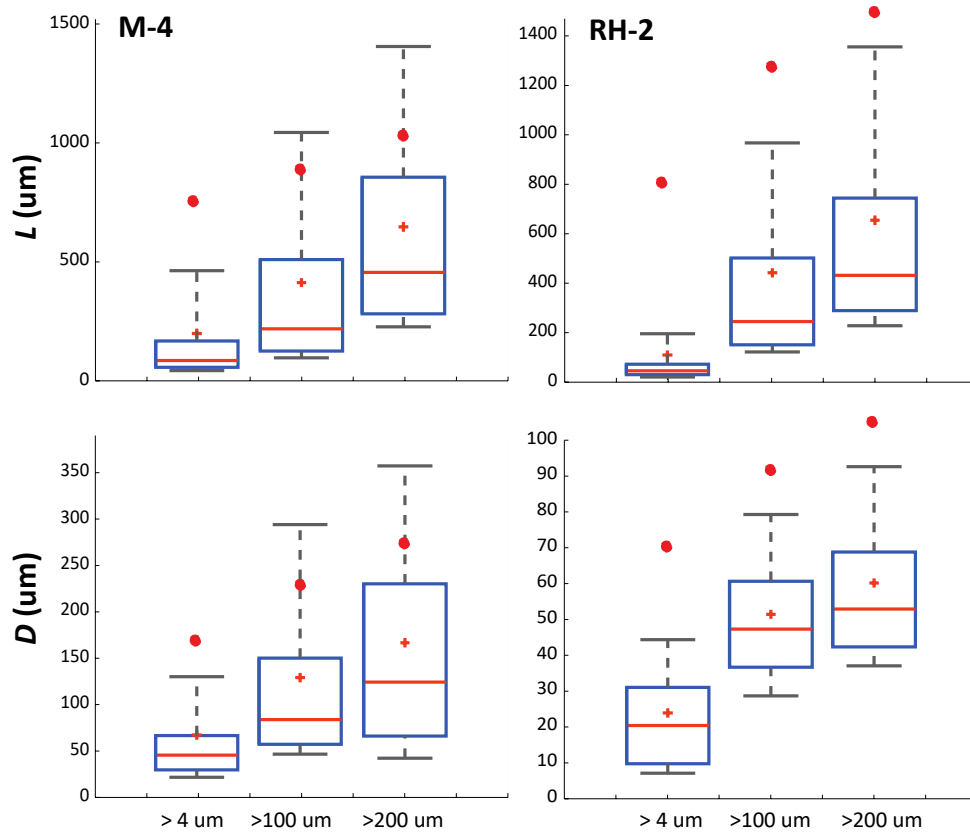


Figure S6

Influence of data range on size distribution. Box-plot for the M-4 (left) and RH-2 (right) samples analyzed through 2D scanner. Three box-plots have been calculated for L (upper) and D (lower) data for three cases: when all data are considered ($> 4 \mu\text{m}$), with a threshold $L_{thres} = 100 \mu\text{m}$ and with $L_{thres} = 200 \mu\text{m}$.



The shape of the distributions and, consequently, their mean, decile and quartile values are strongly influenced and biased by the range corresponding to the measuring method. Figure S6 shows the length and diameter box-plots for miscanthus (left) and retted hemp (right) fibers measured by 2D scanner. Fine particles and short fibers ($L < 100 \mu\text{m}$) represent the majority of the measured elements, i.e. between 62 and 82% for retted hemp samples and between 60 and 66% for miscanthus (see Table 1). This percentage increases up to 80-90% if only fibers shorter than $200 \mu\text{m}$ were considered.

When all elements were counted, the distributions showed a strongly positively skewed shape. The larger the threshold, the lower is the skew and the larger is the IQR. The

mean values, x_n and x_w , systematically increase with the increase of the threshold value, but their difference decreases moderately. In addition, the location parameter, μ , of the log-normal distribution increases with the increase of L_{thres} , i.e. the distribution shifts toward larger values of L and D .

The decrease of the shape parameter, σ , with the increase of L_{thres} , shows the reduction of the degree of skewness of the distribution (Table 1). A σ larger than 1 describes a distribution rising very sharply in the beginning, peaking out early and then decreasing abruptly as an exponential distribution. The prominence of small elements and particles on the length distribution is showed up by $\sigma_L > 1$, for the all fiber typologies (Table 1).

Figure S7

Cartoon describing the cross-section of a non-cylindrical fiber. D_{min} and D_{max} indicate the minor and the major axis of the section, respectively. D_{min} corresponds to the largest circle inscribed in the fiber during the openings method.

